Electroactive Mixtures of Polyaniline and EPDM Rubber: Chemical, Thermal, and Morphological Characterization

S. C. Domenech,[1] J. H. Bortoluzzi,[1] V. Soldi,[2] C. V. Franco[1]

[1]*Laboratório de Eletroquímica e Corrosão, Departamento de Química, Universidade Federal de Santa Catarina, 88040-900 Campus Trindade, Florianópolis-SC, Brazil*
[2]*Grupo de Polímeros, Departamento de Química, Universidade Federal de Santa Catarina, 88040-900 Campus Trindade, Florianópolis-SC, Brazil*

Received 9 October 2001; accepted 18 April 2002

ABSTRACT: A new route for blending polyaniline (PAni) and EPDM rubber was devised with maleic anhydride as a compatibilizer precursor. Rubber matrices containing ammonium peroxidisulfate and dodecyl benzene sulfonic acid were cast from organic solvents. Exposure to the monomer vapors allowed the chemical polymerization of aniline. The influence of PAni and the compatibilizer on the thermal properties, chemical structure, electrical conductivity, and morphology of the mixtures was observed with differential scanning calorimetry, thermogravimetric analysis, Fourier transform infrared, in situ conductivity measurements, and optical microscopy. The micrographs showed a good distribution of the PAni complex in the matrix. The use of approximately 2 wt % compatibilizer resulted in chemical interactions between maleic anhydride and the PAni complex formed with dodecyl benzene sulfonic acid, which could enhance the compatibility between the polymers. The obtained blends reached relative electrical conductivity values of up to 9×10^{-3} S cm^{-1}. © 2002 Wiley Periodicals, Inc. J Appl Polym Sci 87: 535–547, 2003

Key words: blends; conducting polymers; rubber

INTRODUCTION

During the last 20 years, most of the studies concerning conducting polymers have focused on the characterization of these interesting materials to establish a relationship between the chemical structure and related properties. The field has progressed to a level of maturity consistent with a new set of opportunities for developing a wide range of applications based on conducting polymers as materials for industrial products. There has been equally important progress toward a deeper understanding of the basic physics of the π electrons in conjugated polymers. These points came together in recent progress in the area of transport studies of high-quality conductive polymers processed from solution with the introduction of surfactant counterions. High-molecular-weight polyaniline (PAni) has emerged as one of the most promising conducting polymers. Special interest has focused on PAni because of the low cost of the monomer and straightforward high-yield polymerization. Moreover, the conductive form of PAni has excellent chemical stability and relatively high electrical conductivity. Processing high-molecular-weight PAni has remained a difficult task because it has been generally categorized for many years as an intractable material. Melt-processing doped PAni is not possible because the polymer decomposes at temperatures below the softening or melting point. However, some methods have been reported to dissolve and process PAni, without changing the molecular structure of the polymer, in *N*-methylpyrrolidinone,[1,2] in selected amines,[3] or in concentrated sulfuric acid and other strong acids.[4] Despite these earlier advances, the impossibility of doping high-molecular-weight PAni into its conducting form and dissolving the product in common nonpolar or weakly polar organic solvents was long accepted. This problem was solved[5–7] with functionalized protonic acids, which dope and simultaneously render the resulting PAni complex soluble in common organic solvents. A functionalized protonic acid is generally denoted $H^+(M^-—R)$, in which the counterion anionic species contain the R functional group, which is chosen to be compatible with nonpolar or weakly polar organic liquids. Some examples of these acids are D,L-camphor sulfonic acid, dodecyl benzene sulfonic acid (HDBSA), and *p*-toluene sulfonic acid. For HDBSA,

$M^- = SO_3^-$ and R =

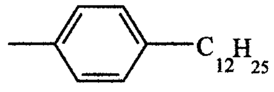

the long alkyl chains of the dodecyl benzene functional group lead to solubility in common solvents,

---

Correspondence to: C. V. Franco (franco@qmc.ufsc.br).
Contract grant sponsor: CNPq.
Contract grant sponsor: CAPES.

Journal of Applied Polymer Science, Vol. 87, 535–547 (2003)

such as toluene, xylene, decalin, and chloroform, and, therefore, render PAni soluble (and processable) in the conducting emeraldine-salt form. MacDiarmid and Epstein[2] reported that free-standing, nonoriented PAni films cast from solvents such as xylene, *m*-cresol, and formic acid have specific electrical conductivities of 100–400 S cm^{-1}, a value 2 orders of magnitude larger than that of doped PAni (e.g., aqueous HCl). However, this large increase in conductivity is not simply due to the nature of the dopant acid employed; it also depends on a suitable dopant–solvent combination to promote conformational changes in the polymer chains and a significant improvement in crystallinity. Some studies[8–12] have been reported on the characterization of a PAni complex formed with HDBSA (PAni–DBSA), which depicts a number of interesting properties, such as thermal stability, high electrical conductivity, and good solubility in organic solvents.

The ability to achieve conducting PAni complexes that are soluble in specific common organic solvents enables the creation of a variety of conducting polyblends in which PAni is blended with bulk polymers. Because counterion-induced processability renders the protonated form of soluble PAni, both PAni and PAni-containing polyblends are processed in the conducting form and, therefore, require no postprocessing chemical treatment. One of the fundamental requirements for creating polyblends is the need for a solvent in which both the conducting PAni complex and the bulk polymer are cosoluble. With such a solvent, conducting polyblends can be made by the codissolution of the polymers at concentrations similar to those cast from solution. The resulting blend will have the desired ratio of conducting PAni complex to bulk polymer. The conductive polyblend material can, therefore, be processed from solution (e.g., fiber spinning, spin casting, and dip coating).[7]

Different strategies have been used to improve the mechanical properties and processability of conductive polymers. Some studies have reported the electrochemical preparation of blends of PAni with Nafion;[13] poly(acrylic esters);[14] and nylon 6.[15] Graft copolymers of PAni and nitrilic rubber[16,17] have also been electrochemically prepared with an organic acid as an electrolyte. The melt processing of PAni doped with HDBSA and polymers such as high-density polyethylene, low-density polyethylene, polypropylene,[18] polystyrene and linear low-density polyethylene[19] has also been reported. In addition, some articles have mentioned the preparation of poly(pyrrole)/EPDM blends[20,21] and, more recently, PAni doped with *p*-toluene sulfonic acid blended with poly(ethylene-*co*-propylene-*co*-diene monomer) by mechanical mixing.[22]

In this study, our interest was focused on the use of PAni and EPDM rubber (an ethylene–propylene–5-ethylidene-2-norbornene terpolymer) to obtain a conductive blend by solution-based methods. The EPDM rubber presents low density, high stability under chemical, atmospheric, and ozone oxidation, and hydrolysis associated with excellent mechanical properties. To enhance compatibility between the polymer components, we employed a compatibilizer precursor. Grafting EPDM rubber with maleic anhydride (MAH) seems to promote the formation of chemical interactions between the PAni–DBSA complex and MAH present in the rubber backbone. Considering the implications that this improvement may have on the properties of the obtained products and on the compatibilization of these mixtures, we found it interesting to carry out a detailed investigation of its chemical structure and properties. Is this article, we report the results obtained by Fourier transform infrared (FTIR), differential scanning calorimetry (DSC), thermogravimetric analysis (TGA), and in situ conductivity measurements. Furthermore, optical microscopy was used to correlate the apparent morphology with the observed properties of the films obtained under various experimental conditions.

EXPERIMENTAL

Reagents and solutions

For the preparation of the polymeric blends, the following chemicals were used: aniline (Aldrich) without previous purification and three kinds of rubber—(1) EPDM (EP57 Nitriflex; 73 wt % ethylene, 27 wt % propylene, and 5 wt % norbornene), (2) EPDM-*g*-$MAH_{0.5}$ (Royaltuf 485, Uniroyal Chemical; modified EPDM rubber with 0.5 wt % MAH functionality), and (3) EPDM-*g*-$MAH_{1.9}$ (EP57 Nitriflex modified with 1.9 wt % MAH functionality; the grafting reaction was carried out according to a procedure outlined elsewhere).[23] $(NH_4)_2S_2O_8$ was used as an oxidant agent. The primary doping of PAni was performed with HDBSA. Xylene was employed for vapor-phase secondary doping. Chloroform or xylene was employed to solubilize the rubber component. In situ direct-current conductivity measurements were performed in a 1*M* aqueous HCl solution containing 0.5*M* LiCl as a supporting electrolyte. All reagents were analytical-grade, and they were purchased from several suppliers.

Blend preparation

The rubber component and the oxidant were primarily milled (Janke & Junkel type A10 analytical mill, IKA Labortechnik) to obtain fine powders. A rubber matrix containing the oxidant agent and the dopant acid was first prepared by the dissolution of 0.2 g of the rubber in 15 mL of the solvent (chloroform for

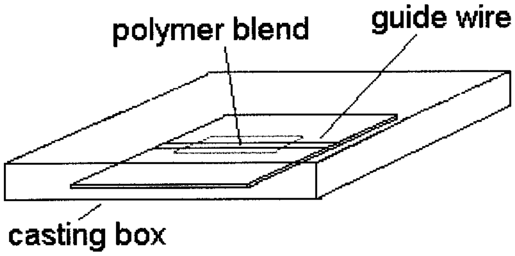

Figure 1 Representative scheme of the polymer blend preparation.

EPDM and EPDM-*g*-MAH$_{0.5}$ and xylene for EPDM-*g*-MAH$_{1.9}$) under mechanical stirring (MQAME-100-MI, Microquímica) at 60°C. A 1*M* HDBSA solution was added to the rubber solution and stirred up to complete the dissolution. Later, the oxidant agent was added and stirred for 30 min. Specimens containing 5, 15, and 25 wt % of each type of oxidant were prepared by the same procedure and with rubbers of different natures. The solution containing the dopant and oxidant was then dip-coated onto a glass sheet and placed into a casting box in a solvent-saturated atmosphere for 24 h. Films 100 μm thick were obtained with a guide wire, as illustrated in Figure 1. For the preparation of the samples for in situ conductivity measurements, 60 μL of the solution was deposited on the surface of a working electrode by dip coating. The final thickness of the film was 30 μm.

The matrix was then exposed to the monomer vapors in a closed, saturated vapor atmosphere for 24 h for the polymerization of aniline. The polymer mixtures cast from chloroform were additionally exposed to xylene vapors for 5 h for vapor-phase secondary doping of PAni. The samples were then stored under a vacuum atmosphere before characterization. The grafting reaction of MAH seemed to change the solubility of the rubber in organic solvents. For this reason, matrices containing EPDM-*g*-MAH$_{1.9}$ were prepared with xylene, in which the rubber could be solubilized.

Blend characterization

DSC was performed on a Shimadzu DSC-50 apparatus. TGA was carried out with a Shimadzu TGA-50 analyzer with samples of approximately 5 mg. The analysis conditions were as follows: aluminum cell, N_2 atmosphere, rate flow = 50.00 mL/min, and rate temperature = 10°C/min. The chemical structures of the polymer components and mixtures were determined by FTIR spectroscopy with a PerkinElmer 16PC apparatus. Thick films (100 μm) of the specimens were employed. The morphology of the polymer blends and the distribution of the conductive polymer in the rubber matrices were observed under a Jenaval–Carl Zeiss optical microscope. In situ direct-current conductivity measurements were carried out in a specially constructed cell containing an internal drying column with highly activated alumina.[24–26] A Pt wire, wrapped around the glass of the working electrode, was used as the counter electrode. The reference electrode was an Ag wire. Potentials were calibrated with ferrocene (Fc) [$E^{+}_{1/2}$(Fc/Fc^{+}) = 0.38 V vs Ag/AgCl/KCl$_{aq}$]. The setup was controlled by an AMEL 553 potentiostat, and the potential scans were performed with an EG&G PAR 175. The working electrode was Pt-sealed in a soft glass (microarray working electrode, 5-μm gap) coated by the polymer blend. The working electrode was separated from the potentiostat by two 1-kΩ resistors[24] (Fig. 2). A bias of $E = 10$ mV was applied to the microarray electrode and a third 1-kΩ resistor at which the potential was measured. The conductivities of the polymers on the electrodes were calculated according to the ohmic rules. The lower limit of the measurable conductivity range was determined by the conductivity of the solvent.

RESULTS AND DISCUSSION

Thermal analysis

DSC thermograms of plain rubber components (second heating run) are shown in Figure 3. All thermograms clearly show the glass-transition temperature (T_g) of the rubber, with the midpoint at −43.4°C for EPDM, at −41.6°C for EPDM-*g*-MAH$_{0.5}$, and at −43.3°C for EPDM-*g*-MAH$_{1.9}$. The ΔC_p values calculated for these processes were 0.703, 0.649, and 0.626 J/gK, respectively. The DSC thermogram of EPDM-*g*-MAH$_{0.5}$ presented some differences compared with

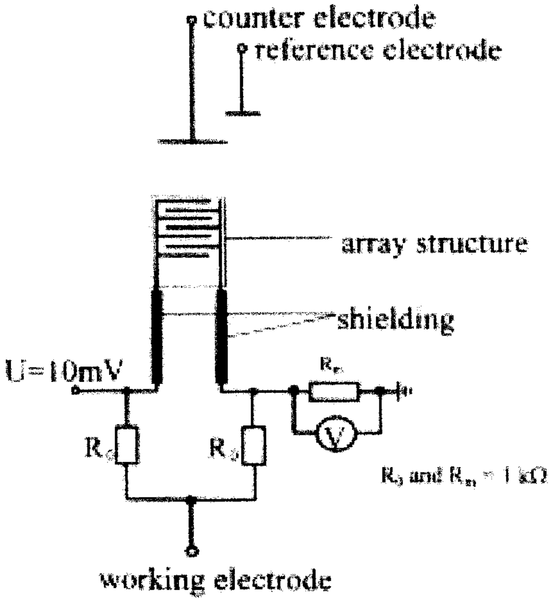

Figure 2 Schematic diagram for the in situ conductivity measurements (electrode width = 5 μm; gap width = 5 μm).[24]

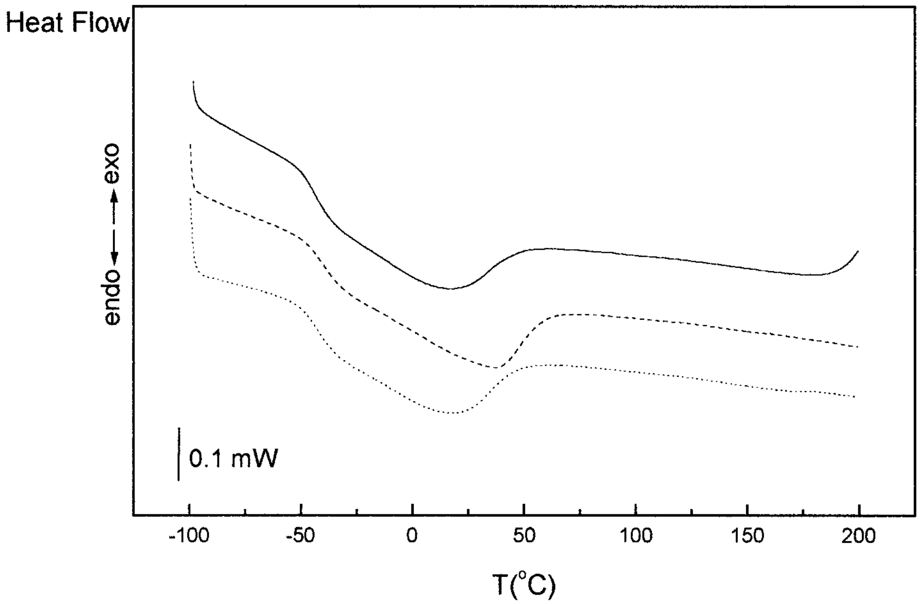

Figure 3 DSC thermograms of (—) EPDM, (–) EPDM-*g*-MAH$_{0.5}$, and (· · ·) EPDM-*g*-MAH$_{1.9}$ rubber.

those obtained for EPDM and EPDM-*g*-MAH$_{1.9}$, as the latter was grafted from EPDM, whereas EPDM-*g*-MAH$_{0.5}$ was a commercial product. Differences in the relative concentrations of ethylene, propylene, and norbornene in the terpolymer could cause T_g of EPDM-*g*-MAH$_{0.5}$ to shift.

The first heating run (not shown in Fig. 3) obtained for these components portrayed either two (or three) endothermic processes related to the melting of the different monomers of the rubber terpolymer, with the maximum peaks at 0.9 and 29.0°C for EPDM, at 10.0, 37.0, and 49.0°C for EPDM-*g*-MAH$_{0.5}$, and at 8.0 and 21.0°C for EPDM-*g*-MAH$_{1.9}$. However, such peaks appear in the second heating run as broad lines after the glass-transition process (Fig. 3). The most reasonable explanation for this comes from the fact that, in the second heating run, the distribution of the crystals in the sample was more homogeneous and the crystal size differences decreased because of the elimination of the thermal history of the sample. The form and particle size of the plain rubbers could not be determined from the preliminary results of a wide-angle X-ray scattering (WAXS) analysis because of the low degree of crystallinity and small crystal size presented by these materials. In addition, ΔC_p of the T_g processes slightly decreased with increasing MAH content. MAH did not significantly affect the degree of crystallinity of the rubber components because of its small concentration in the rubber backbone after grafting.

DSC curves (second heating run) of PAni doped with HDBSA (the PAni–DBSA complex), prepared in chloroform and xylene, are shown in Figure 4. Preliminary results indicated that the DSC thermogram of HDBSA did not show any clear specific thermal behavior below 200°C. This result was in a good agreement with DSC thermograms of HDBSA reported in the literature.[8,18] In the first heating run, endothermic peaks at 55.0, 84.0, and 107.0°C for PAni–DBSA prepared in chloroform and at 54.0, 87.0, and 121.0°C for PAni–DBSA prepared in xylene were observed. Because such peaks were not present in the second heating run, it could be assumed that they were related to water loss, solvent, or low-molecular-weight oligomers present in the samples. In the second heating run, a glass-transition process with midpoints at 82.9 (ΔC_p = 0.218 J/gK) and 79.4°C (ΔC_p = 0.008 J/gK) was observed and corresponded to the PAni–DBSA complexes prepared in chloroform and xylene, respectively. Studies[6,8,9] show that the PAni–DBSA complex presents a phase transition from a pastelike material (with ionic conductivity) to a semisolid material (with electrical conductivity) during the doping process. This transition is a function of the time, temperature, and doping degree. The minimum doping level necessary for its processing is 70% [PAni(DBSA)$_{x=0.7}$].[8] Additionally, the same authors reported that for 1.5 $> x >$ 0.7, T_g of the complex was lower than 150.0°C and decreased when x values increased. For instance, for $x = 0.7$ and $x = 1.5$, T_g was 133.0°C and 65.0°C, respectively. For $x < 0.7$, the values of T_g increased. It could not be defined up to 230.0°C, the onset of polymer degradation. Correlating these findings with the results obtained in this work for PAni–DBSA, we could assume that PAni had a good doping degree and that it was improved with xylene as a secondary dopant. As melting processes were not observed in DSC thermograms, we realized that the melting temperature was higher than the decomposition temper-

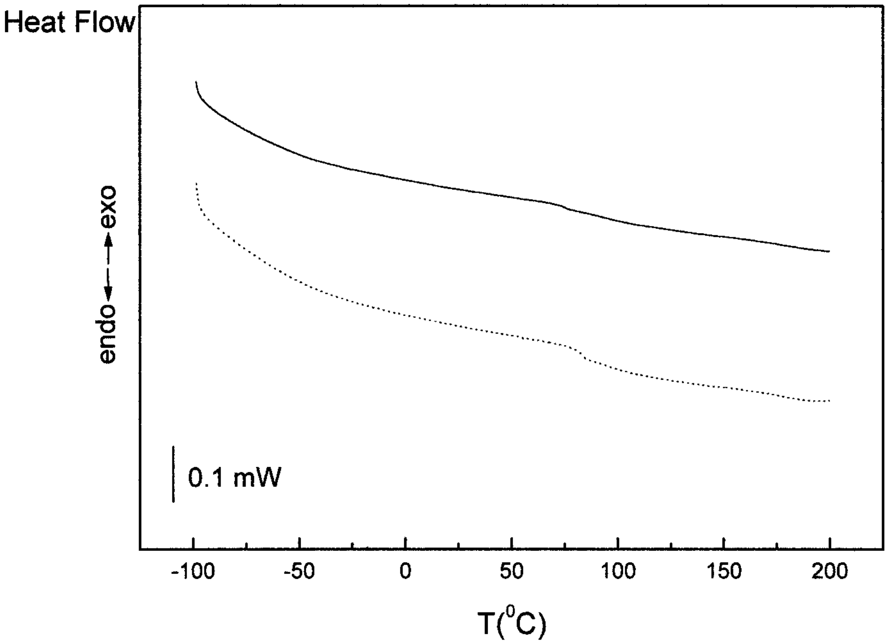

Figure 4 DSC thermograms of the PAni–DBSA complex cast from (—) xylene and (–) chloroform.

atures of both the polymer and dopant. Our preliminary WAXS results indicated that the PAni–DBSA complex was a multiphase crystalline system.

The TGA curves of plain EPDM rubber, EPDM-*g*-$MAH_{0.5}$ rubber, PAni–DBSA cast from chloroform, PAni–DBSA/EPDM, and PAni–DBSA/EPDM-*g*-$MAH_{0.5}$ blends prepared with different concentrations of an oxidant agent are shown in Figure 5(a,b). Figure 6 shows TGA curves of PAni–DBSA blends prepared with rubbers grafted with different concentrations of MAH. Table I lists the temperatures at which the process occurred in each specimen. In the TGA curves of the plain rubber components [Fig. 5(a,b)], a single weight loss related to the decomposition of the rubber was observed. The calculus of the derivative of the TGA curves revealed the presence of only one peak and the shift of MAH mass losses to lower temperatures. In the thermograms of the plain PAni complex [Fig. 5(a,b)], three main weight losses could be observed. The first one, at approximately 124.0°C, corresponded to the loss of water, solvent, or low-molecular-weight oligomers, as observed in the DSC curves of these components. This weight loss was also reported by Zilberman et al.[19] in studies of the thermal behavior of the PAni–DBSA complex. The second one, in the range of 330–335°C, may have stemmed from dopant loss. Kim et al.[11] stated that this weight loss was related to the decomposition of the aliphatic chain of HDBSA, which took place around 250.0°C; this shows that PAni–DBSA is not a simple mixture of PAni and HDBSA. It can then be inferred that a complex formation (i.e., doping reaction) partially occurred. The last mass loss, in the range of 480–500°C and also observed by Zilberman et al., for PAni–DBSA may correspond to changes in the polymer structure, such as crosslinking, followed by the degradation of the polymer (the structural decomposition of the polymer backbone).[11,19] This weight loss has also been assigned to the release of volatile hydrocarbons.

The increasing concentration of PAni–DBSA in the blends slightly decreased the thermal stability of the mixture, as can be seen in Figure 5(a,b). From the TGA curves, different weight losses were observed, depending on the composition of the blend. Blends with high contents of the conducting polymer displayed complex thermodecomposition processes, and the several weight losses observed could be related to the degradation of the rubber and the conducting polymer. The relative increase in the degradation of EPDM and the new weight losses observed with an increasing concentration of the conductive polymer suggested that a higher PAni–DBSA content in the mixtures could induce a higher phase separation between components.[22] This effect was also observed in PAni–DBSA blends obtained with grafted EPDM [Fig. 5(b)].

The effect of increasing the concentration of MAH on the thermal stability of the rubber component and polymer blends can be observed in Figure 6. It is clear that the presence of MAH (~2%) in the polymer backbone slightly reduced the temperature of the thermal decomposition of EPDM rubber. The same effect was observed for the blends produced with EPDM-*g*-$MAH_{1.9}$.

The DSC curves for PAni–DBSA prepared with EPDM, EPDM-*g*-$MAH_{0.5}$, and different concentrations of the oxidant are shown in Figure 7. The DSC curves

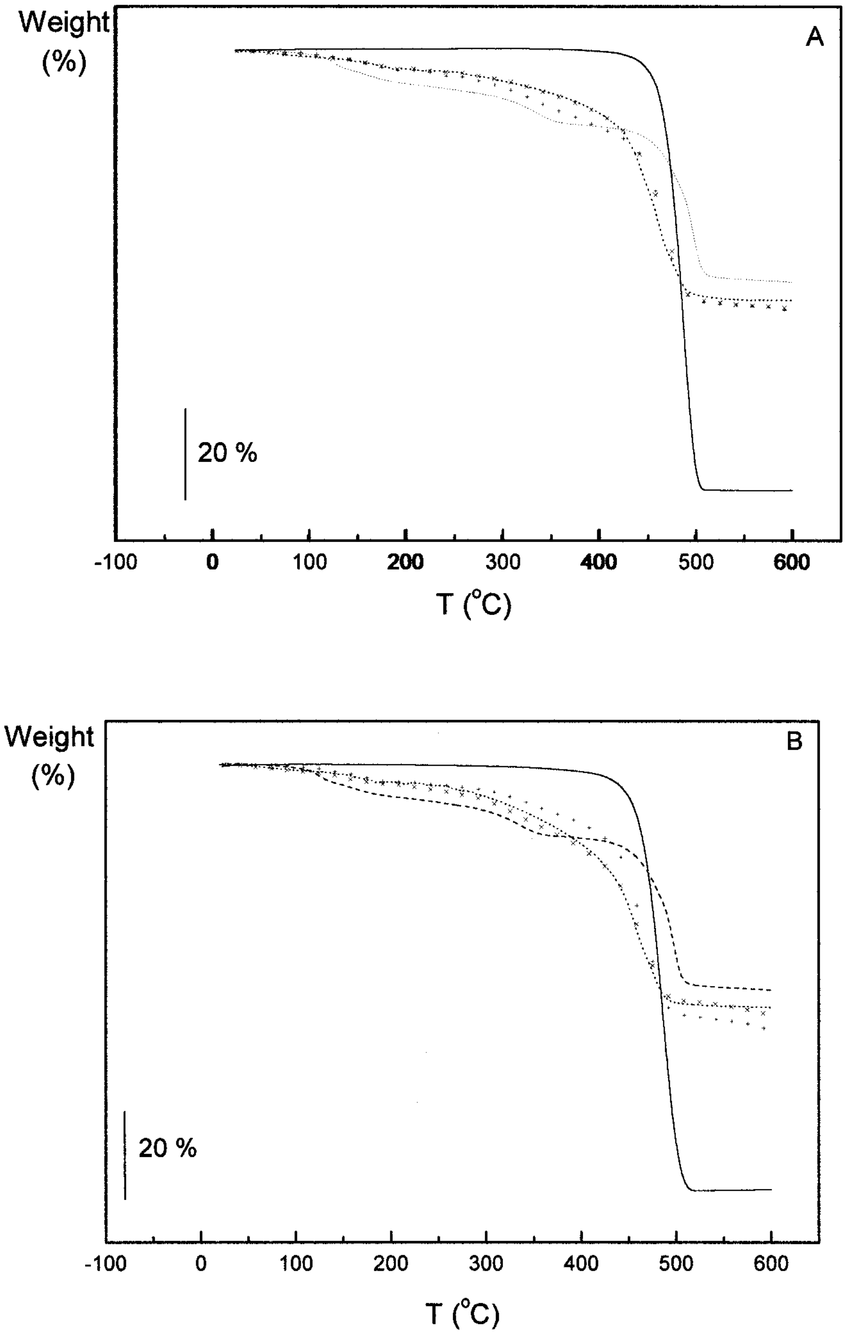

Figure 5 Thermogravimetric curves of (A) (—) EPDM rubber, (–) PAni–DBSA cast from chloroform, and PAni–DBSA/EPDM blends prepared with (·· ·) 5, (×) 15, and (+) 25% $(NH_4)_2S_2O_8$ and (B) (—) EPDM-*g*-$MAH_{0.5}$ rubber, (–) PAni–DBSA cast from chloroform, and PAni–DBSA/EPDM-*g*-$MAH_{0.5}$ rubber blends prepared with (· · ·) 5, (×) 15, and (+) 25% $(NH_4)_2S_2O_8$.

of PAni–DBSA/EPDM blends show the main thermal transitions of EPDM rubber and PAni. The temperatures at which these processes occurred are summarized in Table II. T_g related to EPDM and PAni–DBSA in the blends was slightly shifted with increasing PAni–DBSA content. This effect seemed to be more pronounced in presence of MAH, and this suggested some kind of compatibility between the components in the mixture. A higher concentration of MAH (~2 wt %) was employed to graft EPDM rubber so that we could observe the influence of the concentration of this compatibilizer agent in the polymer mixtures. The shift of T_g of the polymer components was also observed. Figure 8 shows the DSC thermograms of a matrix containing EPDM-*g*-$MAH_{1.9}$, the oxidant agent, and the dopant acid before and after the polymerization of aniline. In the absence of PAni, T_g of the rubber was shifted to −57.0°C, probably because of

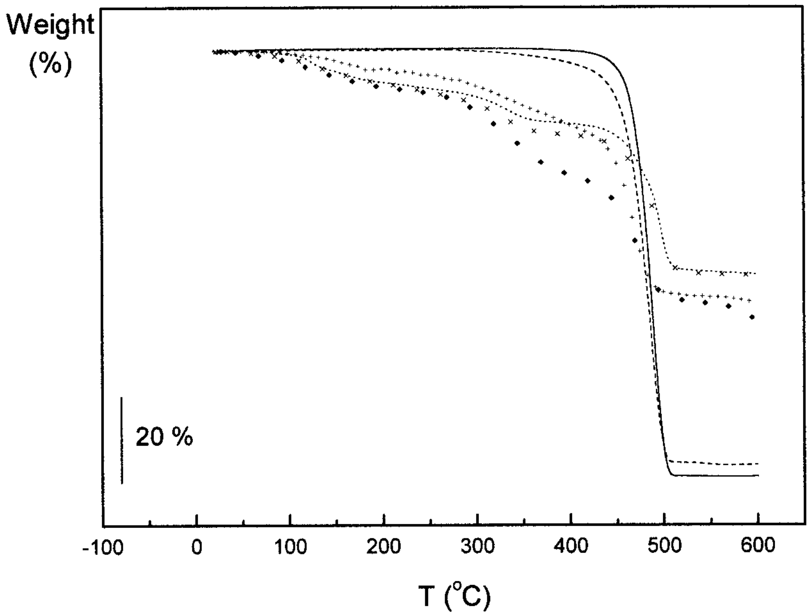

Figure 6 Thermogravimetric curves of (—) EPDM rubber, (–) EPDM-*g*-MAH$_{1.9}$ rubber, (· · ·) PAni–DBSA cast from chloroform, (×) PAni–DBSA cast from xylene, and polymer blends of PAni–DBSA [prepared with 25% $(NH_4)_2S_2O_8$] and (+) EPDM and (◆) EPDM-*g*-MAH$_{1.9}$ rubber.

the presence of MAH. After the polymerization of aniline, it was dislodged to −68°C. The exotherm at 141°C observed in the rubber matrix, related to the oxidation of the rubber component due to the presence of $(NH_4)_2S_2O_8$, was shifted to 92°C when PAni was present. This exotherm, shown in detail in Figure 8, was related to the formation of the PAni–DBSA complex, which was indicated by various authors to occur at 150.0°C.[8,18] The shift to lower temperatures could be due to the presence of MAH in the polymer mixture. The changes in the thermograms were possibly evidence of compatibilization between the polymers and the presence of chemical interactions between MAH and doped PAni.

FTIR analysis

To confirm the existence of chemical interactions between the compatibilizer agent and PAni–DBSA complex in the mixtures, we carried out FTIR analyses (Fig. 9). The main absorption peaks of EPDM rubber grafted with 1.9 wt % MAH can be observed in curve

TABLE I
Weight Losses Observed in TGA Analysis (from Fig. 5 (a, b) and 6)

	Weight loss					
	First loss		Second loss		Third loss	
Specimen	Midpoint (°C)	%	Midpoint (°C)	%	Midpoint (°C)	%
EPDM rubber	489.0	98.9	—	—	—	—
EPDM-g-MAH$_{0.5}$ rubber	486.0	97.7	—	—	—	—
EPDM-g-MAH$_{1.9}$ rubber	415.0	95.9	—	—	—	—
PAni–DBSA (prepared in chloroform)	124.1	7.9	335.8	9.1	498.5	34.8
PAni–DBSA (prepared in xylene)	124.0	10.1	332.1	9.1	491.0	32.7
PAni–DBSA/EPDM blends prepared with						
5% $(NH_4)_2S_2O_8$	125.2	3.7	458.5	61.1	—	—
15% $(NH_4)_2S_2O_8$	124.6	3.9	463.6	63.7	—	—
25% $(NH_4)_2S_2O_8$	123.9	4.4	467.0	64.2	—	—
PAni–DBSA/EPDM-*g*-MAH$_{0.5}$ blends prepared with:						
5% $(NH_4)_2S_2O_8$	139.2	4.3	460.1	36.8	—	—
15% $(NH_4)_2S_2O_8$	135.2	4.8	463.6	28.9	—	—
25% $(NH_4)_2S_2O_8$	130.1	4.2	475.5	30.8	—	—
PAni–DBSA/EPDM-*g*-MAH$_{1.9}$ blends prepared with						
25% $(NH_4)_2S_2O_8$	124.1	9.2	344.1	21.7	473.8	32.0

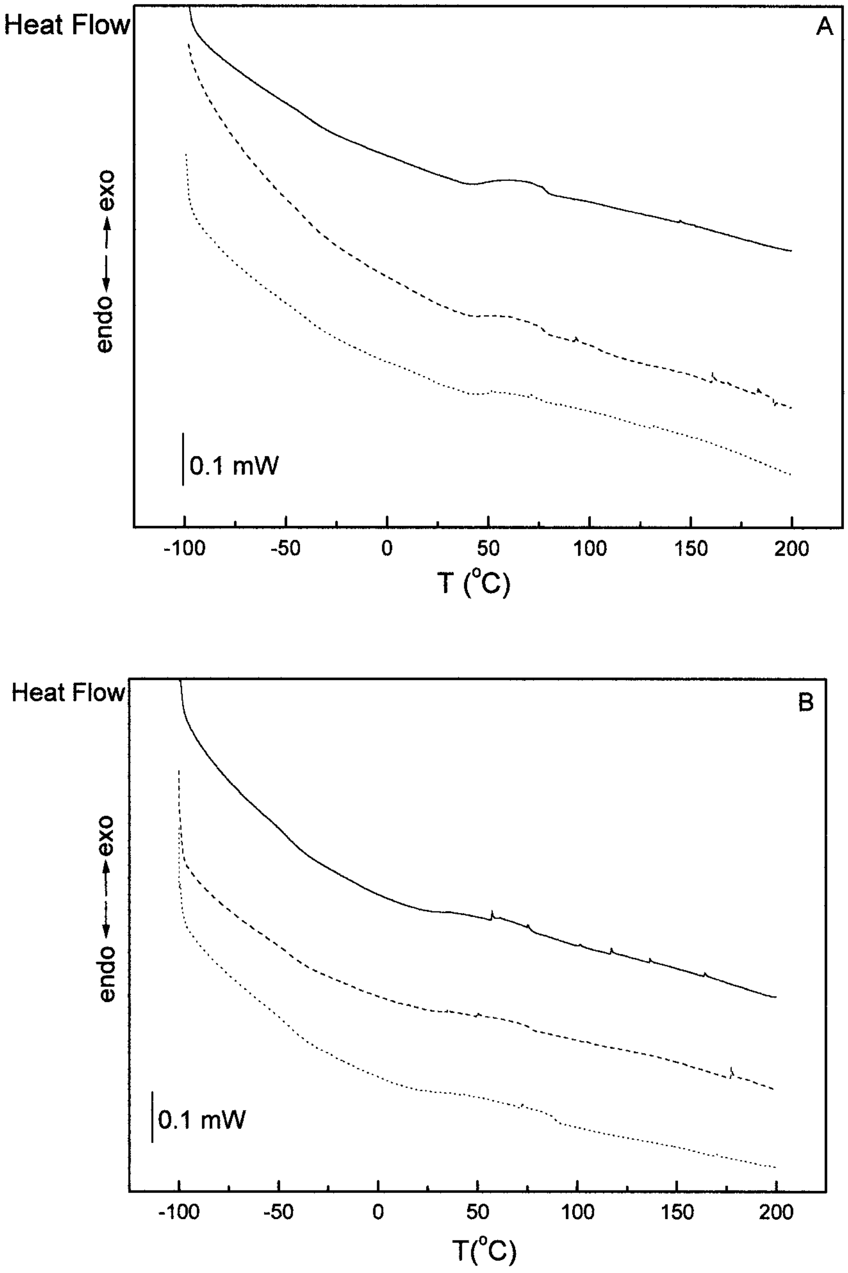

Figure 7 DSC thermograms of (A) PAni–DBSA/EPDM blends prepared with (—) 5, (-) 15, and (· · ·) 25% $(NH_4)_2S_2O_8$ and (B) PAni–DBSA/EPDM-*g*-$MAH_{0.5}$ blends prepared with (—) 5, (-) 15, and (· · ·) 25% $(NH_4)_2S_2O_8$.

A. The (weak) band at 1855 cm^{-1} was attributed to the C═O stretching of MAH, and the peak at 1707 cm^{-1} corresponded to the C═O stretching group of hydrolyzed MAH in grafted EPDM. The band at 922 cm^{-1}, attributed to angular deformation outside the plane of OH bonding, indicated that MAH was incorporated into the EPDM rubber.[23] The other bands, assigned at 2925 and 2850 cm^{-1} (CH stretching), at 1631 cm^{-1} (C═C stretching), at 1460 and 720 cm^{-1} (CH_2 angular deformation), and at 1372 cm^{-1} (CH_3 angular deformation), are typical of EPDM rubber FTIR spectra.[23]

Curve B displays the FTIR spectrum of the PAni–DBSA complex cast from xylene. Characteristic absorption peaks for the usual doped PAni can be observed at 1597, 1459, 1299, and 1121 cm^{-1}.[11]. The absorption band in the range of 3100–3500 cm^{-1}, attributed to the NH stretching, appeared in the pattern as a wide band because of the high concentration of this group in the sample.[27] The weak band observed at approximately 3385 cm^{-1} can be related to OH stretching due to moisture in the sample. Three peaks in the range of 3000–2800 cm^{-1} were attributed to aliphatic groups.[11] The band at 1597 cm^{-1} was assigned to the stretching of quinoid double bonds, and the peak at approximately 1500 cm^{-1} was related to the stretching of benzoid double bonds superimposed

TABLE II
Thermal Transitions of DSC Analysis (from Fig. 7)

Specimen	Thermal transition	
	$T_{g\mathrm{EPDM}}$ (°C)	$T_{g\ \mathrm{PAni}}$ (°C)
PAni–DBSA/EPDM blend prepared with		
5% $(NH_4)_2S_2O_8$	−45.87	71.80
15% $(NH_4)_2S_2O_8$	−50.32	73.02
25% $(NH_4)_2S_2O_8$	−53.80	74.55
PAni–DBSA/EPDM-*g*-$MAH_{0.5}$ blend prepared with		
5% $(NH_4)_2S_2O_8$	−52.92	75.93
15% $(NH_4)_2S_2O_8$	−44.72	80.21
25% $(NH_4)_2S_2O_8$	−45.70	88.32

by other bands. The existence of these bands indicated the emeraldine salt of PAni. The peak at 1459 cm^{-1} could be related to out-of-plane CH wagging, and the band at 1299 cm^{-1} was related to the presence of aromatic secondary amines and is frequently reported in the literature[28,29] as a band with medium intensity in the emeraldine salt or with weak intensity in the emeraldine base. This means that the deprotonation affected the aromatic amines of the polymer. In particular, the intensity of the absorption band at 1161 cm^{-1} increased with doping, and this was considered a measure of the doping level of the polymer backbone.[11] Dhawan and Triverdi[28] described this band as a characteristic of the conductive polymers due to the charge delocalization caused by protonation, and it frequently appeared in the FTIR spectra of the emeraldine salt. Kim et al.[11] reported that the use of PAni–DBSA had some advantages over doped PAni (e.g., with HCl). The peak intensity at 1161 cm^{-1}, a measure of the doping level, slightly increased with heating, and this confirmed that the doping reaction of PAni–DBSA was expedited by heating. Our TGA results indicated that the weight loss of HDBSA from PAni took place at approximately 300–330°C, and this led us to conclude that the PAni–DBSA complex was in the doped state and that its main physical properties, such as the electrical conductivity, solubility, and thermal stability, could be unaffected at temperatures below the dopant degradation.

The peak at 1121 cm^{-1} was assigned to the CN stretching of aromatic amines.[29] Two peaks at 1030 and 1003 cm^{-1} were observed for the PAni–DBSA complex and assigned to the stretching of the S═O bond of HDBSA.[11,30] They are commonly observed in many kinds of sulfonic acid. The vibrations between 650 and 850 cm^{-1} were indicative of CH vibrations on the 1,2,4-substituted rings. The 826-cm^{-1} vibration was the only one to indicate neat 1,4-substituted rings.[30] The appearance of bands at 740 and at 690 cm^{-1} primarily indicated the existence of an asymmetric fraction of monosubstituted rings, that is, lower molecular weight species. However, these two bands might also be representative of some sort of branching on the individual molecules. The bands at 740 and 670

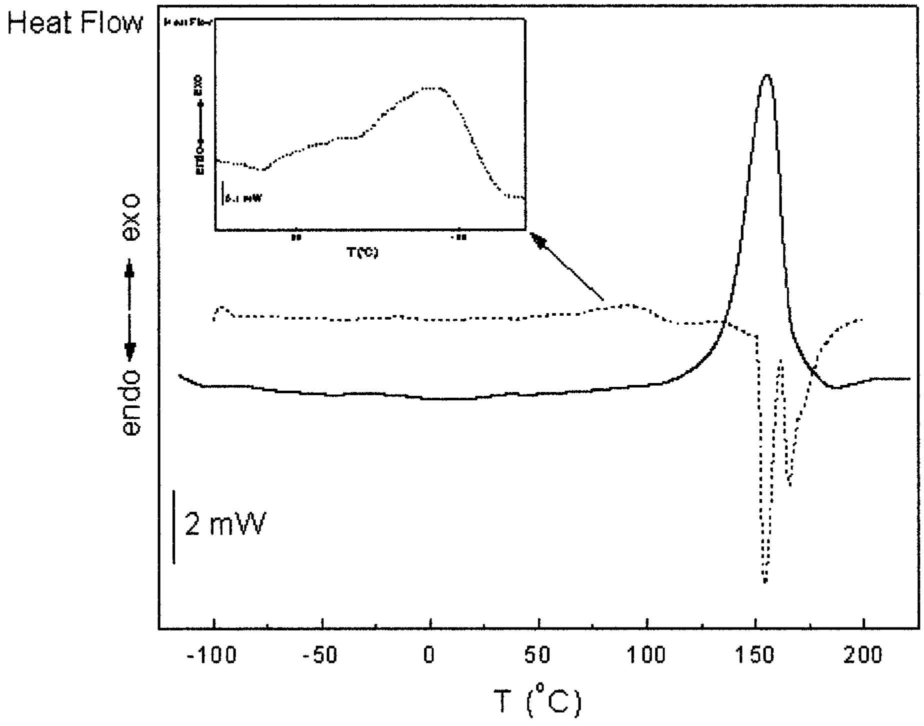

Figure 8 DSC thermograms of a matrix containing EPDM-*g*-$MAH_{1.9}$ rubber, 1*M* HDBSA, and 25% $(NH_4)_2S_2O_8$ (—) before and (–) after aniline polymerization.

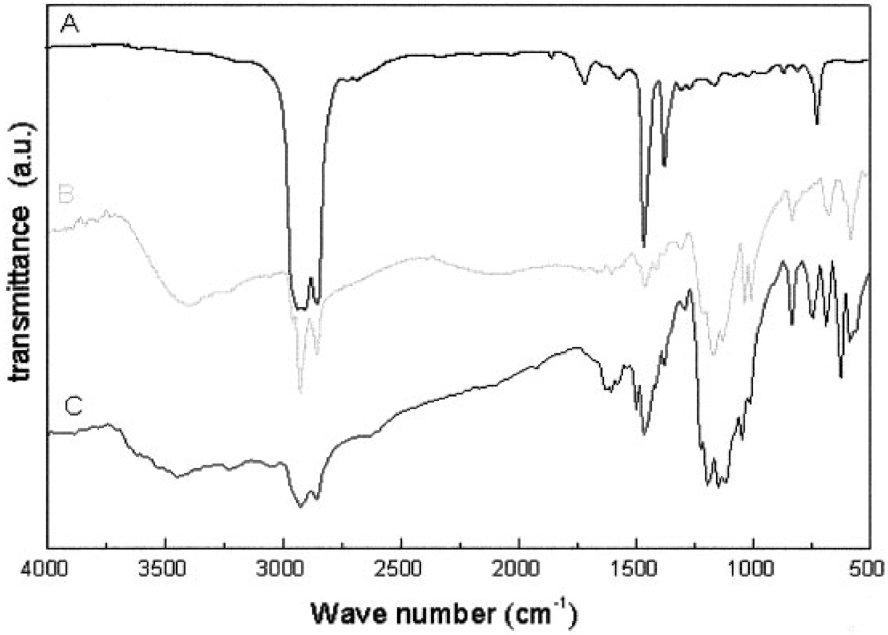

Figure 9 FTIR spectra of (A) EPDM-*g*-MAH$_{1.9}$ rubber, (B) a PAni–DBSA complex cast from xylene, and (C) a PAni–DBSA/EPDM-*g*-MAH$_{1.9}$ rubber blend prepared with 25 wt % $(NH_4)_2S_2O_8$.

cm^{-1} were absent in pattern B. This meant that the concentration of low-molecular-weight species was not significant.

Finally, curve C depicts the FTIR spectrum obtained for a PAni–DBSA/EPDM-*g*-MAH$_{1.9}$ rubber blend prepared with 25 wt % $(NH_4)_2S_2O_8$. This spectrum resembled a superpositioning of the spectra from both polymers. Comparing this spectrum to those of the plain components, we observed nearly the same absorption bands of PAni–DBSA and EPDM-*g*-MAH$_{1.9}$, although there were a few particularities. The absorption bands in the range of 3100–3500 cm^{-1}, attributed to NH or OH stretching,[27] appeared as two absorption bands at 3442 and 3225 cm^{-1} in the spectrum of the blend. These bands could indicate the formation of amide, with amide carbonyl stretching at 1650 cm^{-1} or carboxylic acid stretching at 1713 cm^{-1}.[31] Three peaks in the range of 3000–2800 cm^{-1} were attributed to CH stretching (aliphatic groups) of the PAni–DBSA complex or EPDM rubber. The band at 1707 cm^{-1} present in the rubber spectrum and related to the formation of C═O stretching of carboxylic acid was absent in the blend spectrum, and this indicated the depletion of these groups. The absorption band at 1631 cm^{-1} present in the rubber spectrum and corresponding to C═C stretching was shifted to 1625 cm^{-1} in the blend spectrum. The bands at 1599 and 1493 cm^{-1} were assigned to the stretching of quinoid and benzoid double bonds of PAni–DBSA, respectively. The peak at approximately 1500 was not very clear in the PAni–DBSA spectrum but was present in the polymer mixture spectrum. The peak at 1459 cm^{-1} denoted the out-of-plane C—H wagging of EPDM rubber, and the peak at 1370 cm^{-1} represented the CH_3 angular deformation of EPDM. The band at 1299 cm^{-1}, related to the presence of aromatic secondary amines and usually observed in PAni spectra,[28,29] was also observed in the mixture at 1292 cm^{-1}.

Other peaks in the spectrum of the mixture superimposed the peak at 1161 cm^{-1}. The band at 1121 cm^{-1}, assigned to the CN stretching of aromatic amines,[29] was shifted to 1111 cm^{-1} in the blend spectrum. The two peaks at 1030 and 1003 cm^{-1}, assigned to the stretching of the S═O bond of HDBSA,[11,30] were shifted to 1041 and 1010 cm^{-1} in the spectrum of the polymer mixture. The vibrations between 650 and 850 cm^{-1}, indicative of C—H vibrations on the 1,2,4-substituted rings in PAni, were observed as peaks at 825 and 625 cm^{-1}. The band at 720 cm^{-1}, which represented CH_2 deformation in the rubber backbone, was shifted to 741 cm^{-1} in the blend spectrum.

Studies have shown compatibilizing agents used to produce mixtures between polymers, such as blends of nylon 6 and polypropylene or polystyrene,[32] blends of ethylene–propylene rubber and nylon 6[33] (both with MAH as a compatibilizer), and blends of maleated polypropylene and maleated EPDM by the addition of polyoxypropylene diamine.[31] Observing the spectrum of the polymer mixture in detail, we found evidence for the formation of chemical interactions between MAH and PAni. Because the imine nitrogens of PAni were doped with HDBSA, it was reasonable to assume that the amine nitrogen groups present in the PAni backbone were able to react with MAH grafted in the EPDM rubber. These suppositions were supported by the FTIR spectrum of the blend. The pres-

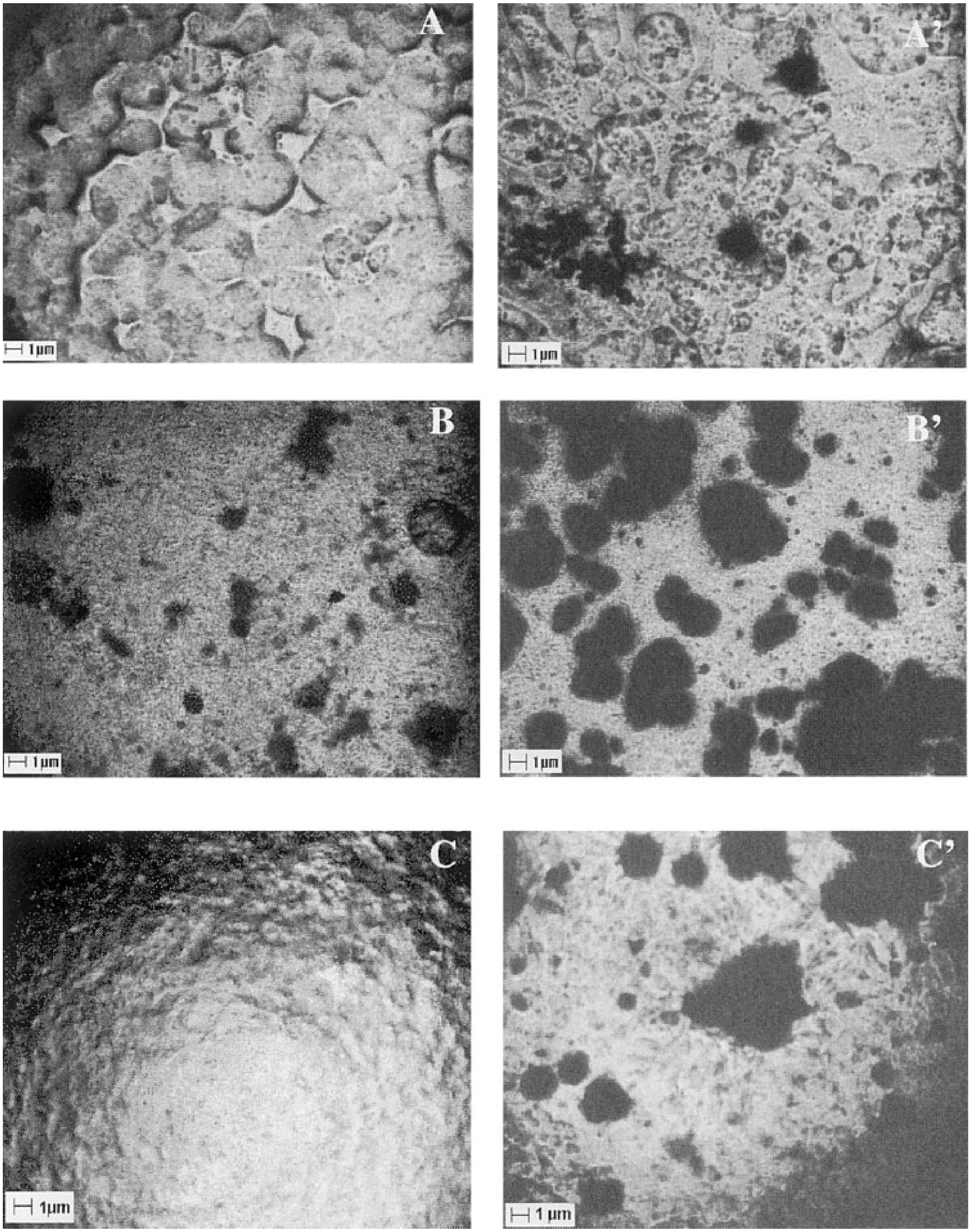

Figure 10 Optical micrographs of the surface of a matrix containing 1*M* HDBSA and 25% $(NH_4)_2S_2O_8$ and (A) EPDM rubber, (B) EPDM-*g*-$MAH_{0.5}$ rubber, and (C) EPDM-*g*-$MAH_{1.9}$ rubber and (A′–C′) matrices A–C after aniline polymerization (magnification, 125×).

ence of the absorption bands in the range of 3100–3500 cm^{-1} could indicate the formation of amide.[31] In addition, the significant reduction in the absorbance of MAH at 1859 cm^{-1} suggested that a reaction of MAH and the amines occurred. The band at 922 cm^{-1}, relative to out-of-plane OH angular deformation related to the MAH incorporated in the rubber, was absent in the blend spectrum. The band at 1707 cm^{-1}, present in

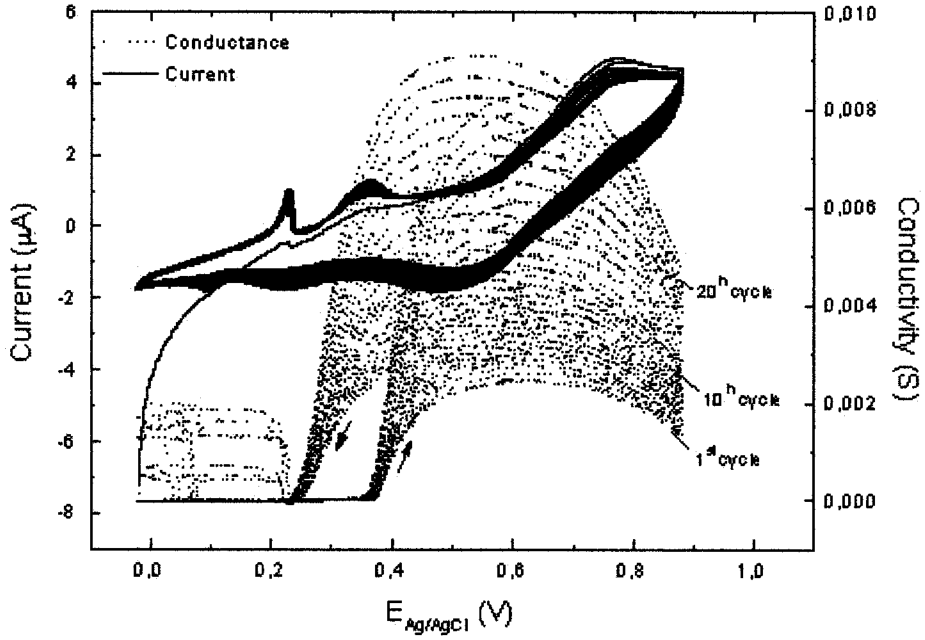

Figure 11 In situ conductivity measurements for the redox cycling of a PAni/EPDM rubber blend prepared with 25 wt % $(NH_4)_2S_2O_8$: (—) cyclic voltammogram and (–) conductivity versus the potential (arbitrary units). $T = 298$ K; $v = 0.001$ V s^{-1}.

the rubber spectrum and related to the formation of C═O stretching of carboxylic acid, was absent in the blend spectrum. This could be an indication concerning the consumption of these groups forming, for example, amide linkages.

Optical microscopy and electrical conductivity measurements

Figure 10 shows the micrographs of rubber matrices containing different types of EPDM rubber. A good distribution of the oxidant particles in the rubber matrix was observed even at lower concentrations. $(NH_4)_2S_2O_8$ formed aggregates with diameters of approximately 1–3 μm. The specimens changed from transparent films to green films after a few minutes of exposure to the monomer vapors. This indicated the formation of PAni in the matrix. Recent studies on electrochemical characterization[34] revealed that all mixtures present electrochemical activity and electrical conductivity. This showed that PAni was formed in the samples obtained by this route. The polymerization of aniline initially occurred preferentially near the oxidant particles, as observed in the micrographs. The presence of MAH in the rubber backbone allowed for a better distribution of the conductive polymer in the rubber matrix. No dramatic differences were observed after secondary doping with xylene. The use of different concentrations of the oxidant did not affect the general aspect of the specimens. Figure 11 illustrates the cyclic voltammogram and relative electrical conductivity of a PAni/EPDM blend prepared with 25 wt % $(NH_4)_2S_2O_8$. Only relative conductivity changes were measured. The polymer film was electroactive, with oxidation and reduction processes relative to PAni present in the rubber matrix. The measured current increased with cycling. The conductivity values also showed an interesting behavior, increasing with the number of cycles, and this suggested that the diffusion of the electrolyte through the blend favored electric contact between PAni particles in the blend. The polymer blends produced with a lower concentration of the conductive polymer presented similar behavior. These promising results have led to a detailed electrochemical study already in preparation.[34]

CONCLUSIONS

The results obtained so far suggest that T_g of EPDM rubber is slightly shifted to lower temperatures because of MAH linked to the rubber backbone. No dramatic changes were observed in DSC curves of the blends prepared with EPDM or EPDM-*g*-$MAH_{0.5}$. The presence of PAni–DBSA and MAH slightly shifted T_g of the polymer components, and this suggested some compatibilization. The results of the thermal analysis of the blends also suggested that some kind of interaction occurred, enhancing the compatibility between the components of the mixture. The FTIR spectrum of PAni–DBSA/EPDM-*g*-$MAH_{1.9}$ resembled a superpositioning of the spectra of both components, with some differences. The absorption bands at 1707 (C═O stretching of hydrolyzed MAH), 1859 (C═O stretching of MAH), and 922 cm^{-1} (OH out-of-plane angular deformation of MAH) were not observed in the IR spectrum of the blend. The presence of bands at 3100–3500 cm^{-1} and at approximately 1650 cm^{-1} could probably indicate some kind of interaction. This evidence indicated that the amine nitrogen groups of PAni could react with MAH to form, for instance, amide linkages. The PAni domains had regular sizes (1–3 μm) and good distribution in the rubber matrix. The presence of MAH seemed to promote homogeneity. The PAni/EPDM rubber blends presented electroactivity and relative electrical conductivities around 10^{-3} S cm^{-1}.

The authors thank Marly Soldi (Departamento de Química, Universidade Federal de Santa Catarina, Brazil) for the thermal analysis and the electrochemistry group of J. Heinze (Universität Freiburg, Germany) for the in situ electrical conductivity measurements.

References

1. Angelopoulos, M.; Asturias, G. E.; Erner, S. P.; Ray, A.; Scherr, E. M.; MacDiarmid, A. G.; Aktar, M.; Kiss, Z.; Epstein, A. J. Mol Cryst Liq Cryst 1988, 160, 151.
2. MacDiarmid, A. G.; Epstein, A. J. Synth Met 1995, 69, 85.
3. Han, C. C.; Shacklette, L. W.; Elsenbaumer, R. L. Meeting of the Materials Research Society, Symposium on Electrical, Optical and Magnetic Properties of Organic Solid State Materials; Boston, 1991; Vol. 6.
4. Andreatta, A.; Cao, Y.; Chiang, J.-C.; Heeger, A. J.; Smith, P. Synth Met 1988, 26, 383.
5. Min, Y.; Xia, Y.; MacDiarmid, A. G.; Epstein, A. J. Synth Met 1995, 69, 159.
6. Mattoso, L. H. C. Quím Nova 1996, 19, 388.
7. Heeger, A. J. Synth Met 1993, 55, 3471.
8. Ikkala, O. T.; Lindholm, T. M.; Ruohonen, H.; Seläntaus, M.; Väkiparta, K. Synth Met 1995, 69, 135.
9. Ashklog, M.; Isotalo, H.; Ikkala, O.; Laakso, J.; Stubb, H.; Osterholm, J. E. Synth Met 1995, 69, 213.
10. Cao, Y.; Smith, P.; Heeger, A. J. Synth Met 1993, 55, 3514.
11. Kim, S.; Ko, J. M.; Chung, I. J. Polym Adv Technol 1996, 7, 599.
12. Titelman, G. I.; Zilberman, M.; Siegmann, A.; Haba, Y.; Narkis, M. J Appl Polym Sci 1997, 66, 2199.
13. Orata, D.; Buttry, D. A. J Electroanal Chem 1988, 257, 71.
14. Lacroix, J. C.; Diaz, A. F. Makromol Chem Makromol Symp 1987, 8, 17.
15. Gregory, R. V.; Kimbrell, W. C.; Kuhn, H. H. Synth Met 1989, 29, 163.
16. Tassi, E. L.; De Paoli, M.-A. Polymer 1994, 33, 2427.
17. Tassi, E. L.; De Paoli, M.-A.; Panero, S.; Scrosati, B. Polymer 1994, 35, 565.
18. Ikkala, O. T.; Laakso, J.; Väkiparta, K.; Virtanen, E.; Ruohonen, H.; Järvinen, H.; Taka, T.; Passiniemi, P.; Österholm, J.-E. Synth Met 1995, 69, 97.
19. Zilberman, M.; Titelman, G. I.; Siegman, A.; Haba, Y.; Narkis, M.; Alperstein, D. J. J Appl Polym Sci 1997, 66, 243.
20. Zoppi, R. A.; De Paoli, M.-A. J Electroanal Chem 1997, 437, 175.
21. Zoppi, R. A.; De Paoli, M.-A. Polymer 1996, 37, 1999.
22. Faez, R.; Gazotti, W. A.; De Paoli, M.-A. Polymer 1999, 40, 5497.
23. Barra, G. M. O.; Crespo, J. S.; Bertolino, J. R.; Soldi, V.; Pires, N. A.; Braz, J. Chem Soc 1999, 10, 31.
24. Smie, A.; Synowczyk, A.; Heinze, J.; Alle, R.; Tschuncky, P.; Götz, G.; Bäuerle, P. J Electroanal Chem 1998, 452, 87.
25. Csahók, E.; Vieil, E.; Inzelt, G. J Electroanal Chem 2000, 482, 168.
26. Smie, A. Von Konjugierten Oligomeren zu Leitfähigen Polymeren—Untersuchung der Redoxzustände, Ladungsspeicherung und Leitfähigkeit; Shaker Verlag: Aachen, Germany, 1997.
27. Neoh, R. A.; Kang, E. T.; Tan, K. L. Polymer 1993, 34, 3921.
28. Dhawan, S. K.; Triverdi, D. C. J Appl Electrochem 1992, 22, 512.
29. Tassi, E. L.; De Paoli, M.-A. Polymer 1992, 33, 24.
30. Rabolt, J. F.; Clarke, T. C.; Street, G. B. J Chem Phys 1979, 71, 4614.
31. Phan, T. T. M.; DeNicola, A. J., Jr.; Schadler, L. S. J Appl Polym Sci 1998, 68, 1451.
32. Ide, F.; Hasegawa, A. J. J Appl Polym Sci 1974, 18, 963.
33. Thomas, S.; Groeninckx, G. Polymer 1999, 40, 5799.
34. Domenech, S. C.; Bortolluzi, J. H.; Costa, I.; Franco, C. V. Electrochemical Characterization of Chemically Prepared Polyaniline/EPDM Rubber Blends; UFSC: Brazil, to appear.